Dynamics of fragment recoil in the femtosecond photodissociation of triiodide ions in liquid solution

Stephan Hess, Helge Bürsing, and Peter Vöhringer

Citation: The Journal of Chemical Physics **111**, 5461 (1999); doi: 10.1063/1.479807
View online: http://dx.doi.org/10.1063/1.479807
View Table of Contents: http://scitation.aip.org/content/aip/journal/jcp/111/12?ver=pdfcov
Published by the AIP Publishing

Dynamics of fragment recoil in the femtosecond photodissociation of triiodide ions in liquid solution

Stephan Hess, Helge Bürsing, and Peter Vöhringer
Max-Planck-Institute for Biophysical Chemistry, Biomolecular and Chemical Dynamics Group, Am Fassberg, D-37077 Göttingen, Germany

(Received 15 April 1999; accepted 22 June 1999)

Novel femtosecond, multiple pulse experiments including polarization control are performed to elucidate the dynamics of fragment recoil in the 400-nm photolysis of triiodide ions in liquid ethanol solution. The instantaneous resonance Raman response of the dynamic system, induced at well defined delays after impulsive bond fission of the parent ion, displays a time-dependent vibrational frequency of the diatomic fragment. This time dependence is interpreted through interactions between the fragments which decay with increasing interfragment separation. Simultaneously, the instantaneous anisotropic response of the reactive system exhibits electronically coherent contributions at very early times after bond breakage and provides direct evidence for the existence of electronic degeneracies in the vicinity of the Franck-Condon region. The decay of this coherent anisotropic component reflects a dynamic lifting of these electronic degeneracies upon recoil of the product species and decay of residual interactions between the fragments. From both experiments it can be concluded that in liquid solution it takes about 2 ps until the fragments arrive in the asymptotic limit of the reaction with negligible product interactions. © *1999 American Institute of Physics.* [S0021-9606(99)51035-0]

I. INTRODUCTION

The role of the solvent environment in affecting elementary chemical processes is a central issue in studying reactive dynamics in condensed media.[1,2] An accurate extraction of those intermolecular interactions that affect reactive nuclear motions of the chromophore (e.g., by exchanging energy and momentum to and from the surrounding bath) is one of the main goals of research devoted to chemical reaction dynamics in liquids.

In particular, the time dependence of these interactions in relation to the fundamental chemical event and the physical nature of the underlying molecular degrees of freedom of the condensed phase system that couple to the reaction coordinate are the most intriguing aspects of chemical reactivity in liquid solution.[3–5] If the time scales for solute motions during the chemical event are distinctly different from those of the solvent the reaction can be described sufficiently by potential energy landscapes that are strictly separable into solute and solvent coordinates. Equilibrium averages of solvent forces exerted along the reaction coordinate can be used if the solvent response is much faster than the reactive motion itself. On the other hand, if the solvent moves considerably slower as compared to the elementary chemical process, the environment is essentially frozen and an average over local solvent structures around the reactants can be used to define chromophore-bath interactions. Such interplays of time-dependent bath response and reactant nuclear motion control the precise nature of the reaction coordinate which, in general, contains a complicated mixture of all possible bath and chromophore nuclear degrees of freedom. In turn, the reaction coordinate defines the mechanism of the chemical process, influences the time scale of its elementary steps, and often times determines the outcome of the overall chemical transformation. Therefore unraveling time-dependent solute-solvent interactions is essential to a comprehensive microscopic understanding of chemical reactions in condensed media.[3–5]

The ultraviolet (UV)/near-UV photodissociation of triiodide in polar solvents provides a suitable model system for the study of various aspects of chemical reaction dynamics in liquid solution.[6–8] The reaction has been shown to occur on a variety of time scales reflecting different elementary dynamical processes that compose the overall chemical reaction. After photoexcitation with ultrashort laser pulses, the initial motion of the system is directed along the symmetric stretching coordinate of the parent ion and leads toward the transition state region of the corresponding iodine/diiodide bimolecular collision.[6–8] This short time evolution can be observed in real time through wavelength-selective probing of coherent wave packet propagation along the nominal reaction coordinate.[9] Subsequent bond breakage and coherent product formation takes place within the first few hundred femtoseconds after impulsive photoexcitation.[6,9] Despite the ultrafast nature of these primary events, it was shown that the surrounding solvent actively participates during these early stages of the reaction and serves to dissipate a significant fraction of excess energy initially delivered by the photolysis pulse.[7]

As evidenced by the band shape stability of the diiodide photoproduct, excess vibrational energy is fully dissipated after 3 ps.[7] The efficiency of vibrational relaxation of the product diatom is extremely enhanced as compared to the corresponding uncharged species I_2 in nonpolar solvents, indicating that long-range solute-solvent coupling dominates

the mechanism for energy dissipation.[10,11] In addition, dynamic symmetry breaking of the chromophore plays a crucial role which represents a highly solvent-specific phenomenon in the condensed phase system.[12,13] It was suggested that deviations from a perfectly centrosymmetric parent molecule strongly influence the degree of vibrational excitation of the diatomic fragment.[13] Recent results on the transient anisotropic response of diiodide ions following bond breakage in triiodide imply that symmetry breaking also affects the early time rotational dynamics of the diatomic product and, therefore, the degree of energy deposition into fragment rotational degrees of freedom.[14] Such experiments also indicate further that, at early times, the bending coordinate can contribute significantly to the reaction coordinate in symmetry breaking solvents. The reaction can be considered complete after approximately 20 ps. This is the typical time scale of diffusive orientational randomization as monitored through time-resolved transient anisotropies with probing of the diatomic fragments. Finally, diffusive rotational reorientation is strongly influenced by solvents which form hydrogen-bonded networks.[14]

Despite these efforts, the dynamics associated with fragment separation and the response of the solvent to the impulsive momentum transfer into the bath upon recoil of the fragments are entirely unclear. The present paper focuses on the time scales associated with translational dynamics of the products in the exit channel for two-body dissociation of triiodide in liquid ethanol solution. Femtosecond, multiple pulse experiments similar to those previously described by Ruhman and co-workers are employed to reconstruct the instantaneous vibrational frequency of the product diatom.[15,16] It will be shown that the vibrational frequency of the future diatom is an accurate mirror image of the fragment interactions which, in turn, are determined by the spatial separation of the product species. The translational dynamics in the exit channel will be discussed using a simple classical, one-dimensional model for fragment recoil in a viscous hydrodynamic continuum.[7] Combining such kinds of experiments with polarization sensitive detection of the probe pulse gives access to details regarding the electronic structure of the dynamically evolving system.[17,18] Specifically, the decay of product interactions with increasing interfragment distance gives rise to time-dependent modifications of the electronic structure of the system which manifest themselves in the decay of electronically coherent contributions to the instantaneous anisotropy of the system.

II. EXPERIMENT

The experiments were performed with a home-built Ti:sapphire oscillator/regenerative amplifier system that is capable of generating 30-fs optical pulses at 800 nm with an energy of 0.5 mJ at repetition rates of 1 kHz.[7] Optical pulses at a wavelength of 400 nm with a duration of 30 fs were produced by frequency doubling in a 0.1-mm thick type-I BBO crystal. The fundamental and second harmonic pulses were sent into a photolysis-pump-probe arrangement schematically shown in Fig. 1.

The 400-nm pulses were picked off by a dichroic beam splitter and sent to a computer controlled translation stage.

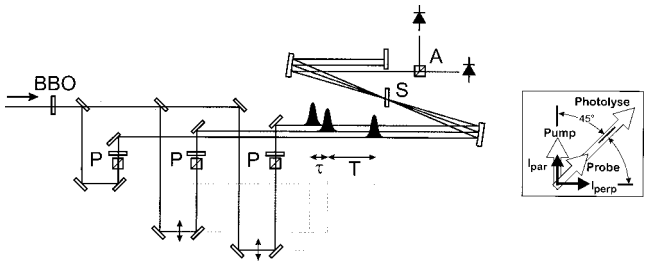

FIG. 1. Experimental configuration for the measurement of the instantaneous resonance Raman response and the instantaneous anisotropy response of diiodide ions following photodissociation of triiodide. BBO: frequency doubler, P: combination of Glan-Taylor polarizers and half-wave retardation plates, S: sample, A: analyzer, T: photolysis-pump-delay, τ: pump-probe delay. The inset emphasizes the polarization conditions for photolysis, pump, and probe pulses.

the residual 800-nm pulses were attenuated, divided into pump and probe pulses by a 50% beamsplitter, and also sent to individual optical delay lines. The relative polarization of the photolysis and pump pulses was set to 45 deg using Glan-Taylor polarizers and zero-order half-wave retardation plates. For instantaneous anisotropy experiments, the polarization vector of the probe pulse was aligned parallel to the photolysis pulse. All pulses were temporally and spatially overlapped in the sample using all-reflective optics with a radius of curvature of 1 m. Behind the sample, a Wollaston prism polarizer was used to separate those components of the probe light which were polarized parallel and perpendicular with respect to the *E*-field vector of the pump. For each laser shot, the intensities I_{par} and I_{perp} of both components were detected simultaneously, together with the reference intensity in front of the sample. The instantaneous anisotropy at photolysis-pump-delay T and pump-probe time delay τ was calculated from successive laser shots according to

$$r(\tau,T)=\frac{\Delta \mathrm{OD}_{\mathrm{par}}(\tau,T)-\Delta \mathrm{OD}_{\mathrm{perp}}(\tau,T)}{\Delta \mathrm{OD}_{\mathrm{par}}(\tau,T)+2\Delta \mathrm{OD}_{\mathrm{perp}}(\tau,T)}=\frac{1-\rho}{1+2\rho}. \quad (1)$$

Here, $\Delta \mathrm{OD}_{\mathrm{par,perp}}$ denotes the pump-induced optical density detected parallel/perpendicular with respect to the pump pulse polarization and the polarization ratio ρ is defined as $\Delta \mathrm{OD}_{\mathrm{perp}}/\Delta \mathrm{OD}_{\mathrm{par}}$. Since the polarization of both probe components is oriented at 45 deg with respect to the polarization of the photolysis pulse, the anisotropy given by Eq. (1) carries contributions that are only induced by the pump field. Anisotropic contributions that are induced by the linearly polarized photolysis pulse are entirely suppressed.

For measurements of the transient resonance impulsive stimulated Raman response of the sample, the probe pulses were polarized parallel with respect to the pump pulse polarization. Also, the Wollaston prism polarizer was removed from the probe beam path, thereby recording the pump-induced optical density $\Delta \mathrm{OD}_{\mathrm{par}}$. Saturation was tested for by monitoring the maximum anisotropy while continuously decreasing the excitation density until the pump-induced optical density has completely disappeared. Triiodide solutions in ethanol with a concentration of 3 mM were prepared according to Ref. 7. All chemicals were obtained from Aldrich and were used without further purification.

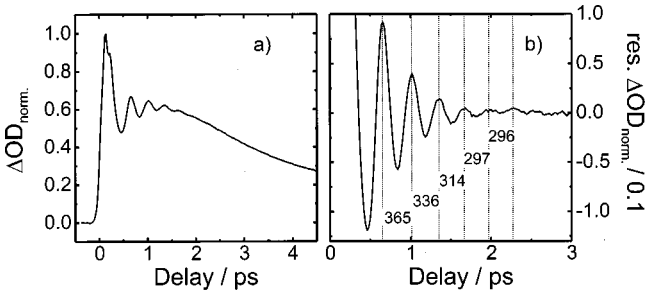

FIG. 2. (a) Conventional pump-probe signal of a triiodide solution in ethanol with photolysis at 400 and detection at 580 nm. (b) Wave packet contribution obtained from (a) after subtraction of the nonoscillatory incoherent contribution to the transient absorption. The numbers indicate the wave packet period estimated from the maxima.

III. RESULTS

A. Transient absorption in conventional pump-probe

Triiodide ions in liquid polar solutions show a very characteristic absorption spectrum in the near-UV spectral region which is a superposition of two strong resonances centered at 280 and 360 nm, respectively.[19] Photoexcitation into either of these bands results in direct photodissociation with formation of diiodide ions in their electronic ground state ($^2\Sigma_u^+$) within the first few hundred femtoseconds.[6,9] Diiodide ions in polar liquids also exhibit two broad absorption bands centered near 400 and 740 nm, respectively.[20] The formation of the diatomic product ions upon ultraviolet irradiation of triiodide can thus be monitored through conventional femtosecond transient absorption measurements with resonant probing in the visible spectral region.

A representative short-time optical pump-probe response of triiodide dissolved in ethanol solution is shown in Fig. 2(a) for excitation at 400 nm and probing of the I_2^- product at 580 nm. The signal displays an ultrafast absorption spike which can be assigned unambiguously to the Franck-Condon region and the transition state region of the corresponding iodine/diiodide bimolecular collision. Such an assignment is based on the results of our previous studies on the 266-nm photolysis of I_3^- in which specific resonant probe windows were spanned along the symmetric stretching coordinate of the reactive system.[9]

Subsequent to this ultrafast feature, the transient absorption slightly increases until a delay of approximately 2 ps with a typical time constant of several hundred femtoseconds independent of the probe wavelength. We have recently assigned this behavior tentatively to the appearance of the fragments in the asymptotic limit of the reaction. This interpretation rests on the excitation energy dependence of this feature we reported previously.[9] Using a shorter photolysis wavelength results in a more pronounced evolution of the system along the symmetric stretching coordinate. Consequently, the system is out of resonance with the probe laser for a longer time before it arrives in the exit channel for diiodide formation where another resonant probe window exists. As a result, the minimum of the transient absorption around 500 fs is much more pronounced and the rise is significantly delayed from the initial spike when using a shorter pump wavelength.

On even longer time scales, the probe wavelength dependence of the transient absorption becomes highly complex. Close to the center of the diiodide optical resonance, the transient absorption levels off until it starts to increase again with time constants of several picoseconds. In parallel, the transient absorption decreases on identical time scales if the probe wavelength is located at the high and low energy edges of the diiodide absorption spectrum. The long time window is dominated by fragment vibrational relaxation which competes with the fast components of geminate recombination. This interpretation is supported by a reconstruction of instantaneous incoherent absorption spectra of diiodide product ions.[7]

Superimposed on these zero-frequency signal contributions, distinct oscillations can be observed for delays below 2 ps. They signify a high degree of vibrational coherence in the product diatom which originates from the ultrafast nature of the optical excitation process.[6] Subtracting the incoherent, nonoscillatory background of the signal and expanding the residual vibrational coherence reveals chirped wave packed dynamics similar to those we previously reported for the 266-nm photolysis.[9] The time dependence of the product vibrational period is emphasized in Fig. 2(b). The origin of this chirped wave packed motion is the major focus of this paper.

B. Transient resonance impulsive stimulated Raman scattering

To further explore the origin of chirped wave packed dynamics detected in conventional pump-probe experiments and to obtain more accurate information about the temporal evolution of the vibrational frequency of the diatomic fragment, resonant impulsive stimulated scattering experiments[15,16] have been performed for well defined delays after impulsive 400-nm photolysis of the parent triiodide ions. Triiodide is photolyzed at time $t=0$ with a 30-fs, 400-nm pulse. At $t=T$, a 30-fs, 800-nm pump pulse induces a Raman excitation of the nascent diiodide product ions. For $T\rightarrow\infty$, this pulse is exactly on resonance with the ($^2\Pi_g \leftarrow ^2\Sigma_u^+$) transition of equilibrated I_2^- product ions.[21] On the other hand, for $T\rightarrow 0$, the same pulse is on resonance with higher lying electronic configurations of triiodide and of the transition state region that give rise to early time transient absorptions in a conventional pump-probe configuration with probing in the visible/near infrared (IR) spectral region [see Fig. 2(a)].[9] The pump-induced vibrational coherence (due to resonance Raman excitation[22]) and transient bleach (due to nonlinear absorption[22]) prepared at time T is finally detected for variable pump-probe time delay τ with a second electronically resonant 30-fs 800-nm pulse (hereafter referred to as probe pulse). For $\tau\rightarrow 0$, this probe pulse utilizes the same electronic transition that is involved in the pump process. Note that this is not necessarily the case for $\tau\rightarrow\infty$.

Figure 3 illustrates representative I_3^-/I_2^- resonance Raman/nonlinear absorption responses along the τ-delay for photolysis-pump delays T ranging between 40 fs and 20 ps. As expected, the data are highly oscillatory along τ and provide a wealth of information about the instantaneous vibra-

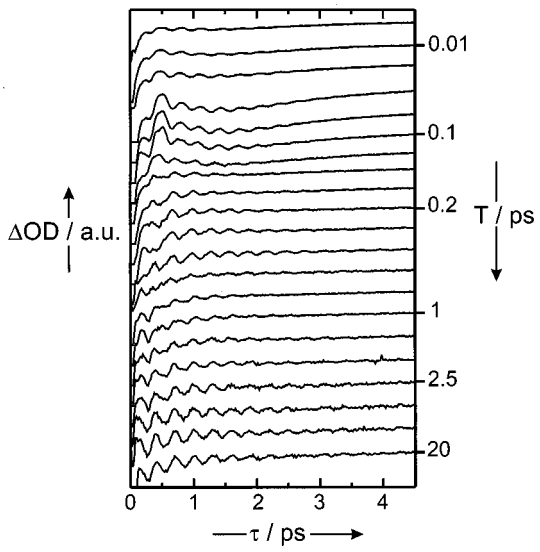

FIG. 3. Instantaneous resonance Raman/nonlinear absorption of the triiodide/diiodide system following impulsive 400-nm photolysis of triiodide in ethanol solution for various photolysis-pump delays ranging between 40 fs and 20 ps. Pump and probe wavelengths were 800 nm. The photolysis wavelength was 400 nm.

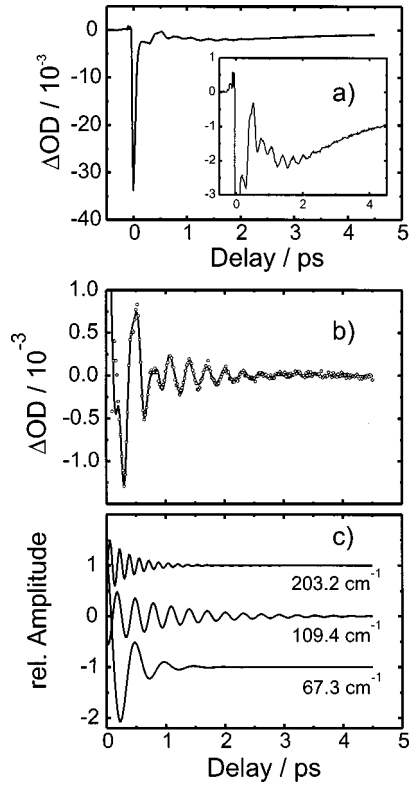

FIG. 4. Instantaneous resonance Raman/nonlinear absorption of triiodide in ethanol solution at a photolysis-pump delay of $T=100$ fs: (a) Optical density as a function of pump-probe time delay τ. (b) Linear-prediction singular-value-decomposition of the oscillatory contribution to the data shown in (a). The solid curve displays the overall fit to the experimental data (open circles). (c) Individual frequency components that compose the overall LPSVD fit.

tional frequencies of the I_3^-/I_2^- system during the photodissociation process. The data were analyzed by performing a linear prediction singular value decomposition (LPSVD) in terms of exponentially damped cosinusoids,[23,24]

$$S(\tau,T)=\sum_i A_i(T)\cos[\omega_i(T)\tau+\phi_i(T)]\exp\left(-\frac{\tau}{\Gamma_i(T)}\right). \quad (2)$$

Such an analysis reveals the amplitudes $A_i(T)$, damping constants $\Gamma_i(T)$, frequencies $\omega_i(T)$, and phase angles $\phi_i(T)$ of all oscillatory components as a function of photolysis-pump time delay T, i.e., as a function of time after impulsive photolysis of triiodide ions. Figure 4 exemplifies the data processing for the instantaneous Raman/bleach response of the I_3^-/I_2^- system for a delay of $T=100$ fs. Three frequency components can clearly be distinguished, two of which show frequencies of around 100 and 200 cm^{-1}, respectively. They seem to agree rather well with the fundamental and the first overtone of the diiodide vibration, whose harmonic frequency is known to be 113 cm^{-1} in liquid solution.[25] Interestingly, a third low-frequency component around 70 cm^{-1} is uncovered which is damped extremely rapidly with a time constant of about 200 fs. Its origin is unclear so far. As a test for reliability of the LPSVD analysis, the data were Fourier transformed after subtraction of the nonoscillatory bleach component. The Fourier spectrum corresponding to a photolysis-pump delay of 100 fs is reproduced in Fig. 5. Again, all three components can clearly be identified whose frequencies agree quantitatively with those obtained through the LPSVD analysis. In addition, their spectral width is in agreement with the dephasing times obtained through LPSVD analysis.

The T-dependence of the frequencies of the fundamental, the first overtone, and the low-frequency component is displayed in Fig. 6. The fundamental shows only a moderate dependence on the photolysis-pump delay. With increasing T, the fundamental asymptotically approaches a value of 113 cm^{-1}, as expected for equilibrated diiodide ions. Simultaneously, the first overtone assumes a value of 220 cm^{-1} for infinite photolysis-pump delays in correspondence with the temporal evolution of the fundamental. The low-frequency component, however, exhibits a very pronounced T-dependence. For very early delays around $T=50$ fs, it can

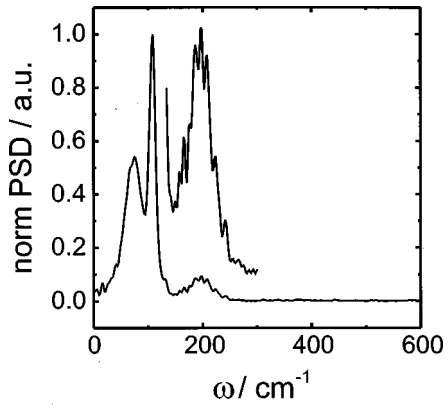

FIG. 5. Fourier power spectral density of the experimental resonance Raman response shown in Fig. 4 after subtraction of all nonoscillatory components to the data. Three frequency components can be identified which agree very well with the results of the LPSVD analysis (see Fig. 4).

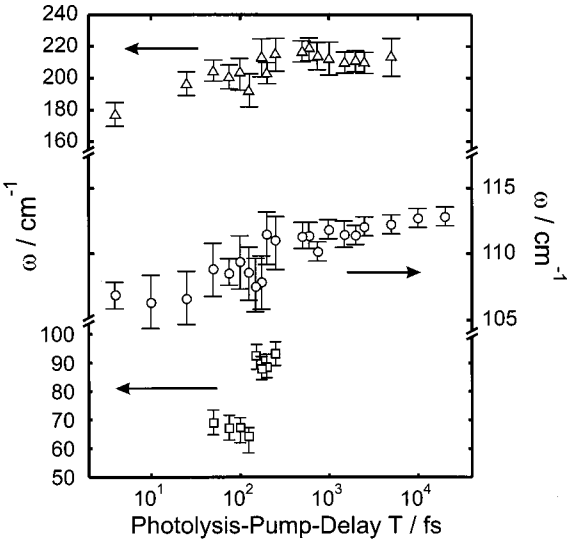

FIG. 6. Vibrational frequencies as a function of photolysis-pump delay T obtained from an LPSVD analysis of the instantaneous resonance Raman response of triiodide solutions in ethanol following photolysis at 400 nm.

be detected at frequencies close to 65 cm^{-1}. It sharply rises with increasing T until it finally merges with the fundamental for photolysis-pump delays around $T=1$ ps. These results will be discussed in the next section in terms of the fragment recoil motion in the exit channels for diiodide formation.

C. Instantaneous anisotropy

The experiments reported in the previous subsection can also be carried out with polarization sensitive detection of the probe as described in Sec. II. Such a detection scheme allows for a measurement of the instantaneous pump-induced anisotropy $r(\tau,T)$ of the system.[26] The instantaneous anisotropy is defined as the correlation function of the scalar product of pump and probe transition dipoles at the instant T of the pump following the impulsive photolysis of I_3^-,

$$r(\tau,T)=\frac{1}{5}\langle P_2[\mu_{\mathrm{Pump}}(\tau=0,T)\mu_{\mathrm{Probe}}(\tau,T)]\rangle$$

$$=\frac{2}{5}\langle P_2[\cos\theta]\rangle. \qquad (3)$$

Here, θ is the angle between the transition dipole of the pump transition at time $t=T$ and that of the probe transition at time $t=T+\tau$.

In the limit of infinite T, both pump and probe transition dipoles are oriented parallel with respect to each other and are associated with the $(^2\Pi_g \leftarrow {}^2\Sigma_u^+)$ resonance of equilibrated I_2^- ions.[21] Hence, for $T\rightarrow\infty$ and a vanishing pump-probe time delay, a maximum anisotropy of 0.4 is expected for a pump-probe time delay $\tau=0$. The decay of $r(\tau,\infty)$ along τ should contain a long time exponential decay which is determined by the rotational diffusion time constant of equilibrated diiodide ions. On shorter pump-probe delays, an inertial component should be recovered whose decay is determined by the rotational correlation time τ_c of diiodide ions.[14,27] This, in turn, is given solely by the rotational temperature of the system at time $t=T$ (e.g., 300 K for $T\rightarrow\infty$) and the moment of inertia Θ of I_2^- according to $\tau_c=(\Theta/3k_BT)^{1/2}$. From conventional anisotropy data on the 400-nm photolysis of triiodide, it is known that the process of bond breakage leads to a substantial degree of fragment rotational excitation of up to 800 cm^{-1} in ethanol solution.[14] By measuring $\tau_c(T)$ as a function of photolysis-pump-time delay T through detection of the inertial contribution to the instantaneous anisotropy decay, the dynamics of rotational energy relaxation can, in principle, be recorded.

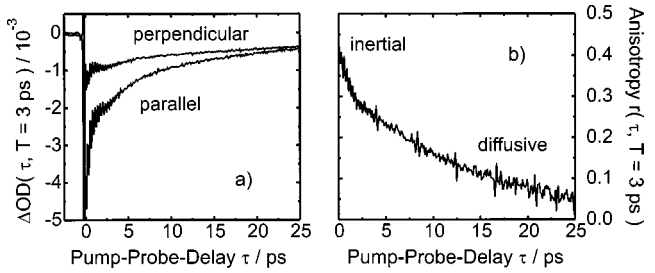

FIG. 7. (a) Pump-induced parallel and perpendicular optical densities as a function of pump-probe time delay τ detected at a photolysis-pump delay T of 3 ps. (b) Corresponding instantaneous anisotropy $r(\tau,T=3$ ps) displaying the typical inertial and diffusive behavior for short and long pump-probe delays, respectively.

In the other limit, for vanishing photolysis-pump delays (i.e., $T=0$), the system is localized on the reactive potential energy surface close to the Franck-Condon region for photolysis and close to the transition state region for the bimolecular I_2^-/I full collision. Here, the pump pulse induces an anisotropy utilizing optical transitions to higher lying electronic configurations of the system that give rise to early time transient absorptions seen in conventional pump-probe (see Fig. 2). Although the precise nature of such resonances is not known at this stage, a maximum anisotropy for vanishing pump-probe time delay of 2/5 should be expected since pump and probe frequencies are degenerate and the associated transition dipole moments are identical.

Figure 7 displays the parallel and perpendicular pump-induced optical densities and the corresponding instantaneous anisotropy of the I_3^-/I_2^- system for a photolysis-pump delay of 3 ps, i.e., for a delay of 3 ps after impulsive photolysis of triiodide. Indeed, $r(\tau,3$ ps) decays exponentially for long pump-probe time delays with a time constant of 12 ps. This value is in excellent agreement with the rotational diffusion time constant of diiodide we reported earlier.[14] For shorter τ-delays the inertial component can be recovered as expected. It reveals a Gaussian correlation time of 900 fs, indicating that fragment rotational excess energy is fully relaxed for delays of $T=1$ ps after impulsive I_3^--photolysis. A full account on the dynamics of rotational energy dissipation in the I_3^-/I_2^- system will be presented in a future publication. Finally, we observe an initial (i.e., $\tau=0$) anisotropy of 0.4 as expected for parallel pump and probe transition dipoles.

Shortening the photolysis-pump-delay T below 1 ps dramatically influences the behavior of $r(\tau,T)$ along τ, as demonstrated in Fig. 8 for $T=500$ fs. First, $r(\tau,T=500$ fs) is not a monotonically decaying function of τ. It rather exhibits a singularity around a pump-probe time delay of approxi-

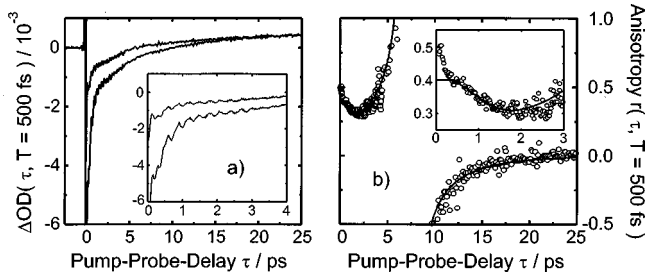

FIG. 8. (a) Pump-induced parallel and perpendicular optical densities as a function of pump-probe time delay τ detected at a photolysis-pump delay T of 0.5 ps. (b) Open symbols: corresponding instantaneous anisotropy $r(\tau, T=0.5$ ps) which exhibits a singularity around $\tau=8$ ps due to opposite signs of the pump-induced optical densities at this pump-probe time delay. The solid curve corresponds to a model which includes the interfragment distance dependence of the transition moment (see Appendix).

mately 8 ps. At this delay, parallel and perpendicular optical densities have opposite signs and the polarization ratio ρ becomes $-1/2$ [see Eq. (1)]. Both transients show a transient bleach for early τ-delays and a transient absorption on longer time scales, indicating that the 800-nm absorption cross section of the system at the instant of the pump is smaller than that of equilibrated diiodide ions (see Appendix). More importantly, however, we note that the initial anisotropy (i.e., $\tau=0$) shown in Fig. 4(b) significantly exceeds the value of 0.4 predicted for parallel pump and probe transition dipoles.

The complete T-dependence of the initial anisotropy has been measured by scanning the photolysis-pump delay with respect to the pump-probe sequence whose interpulse delay has been held constant at 40 fs. The result of such a measurement is reproduced in Fig. 9. Immediately after photolysis, i.e., for $T=0$, the instantaneous anisotropy exhibits a maximum value of 0.7. Subsequently, it decays with increasing T-delay to a value of precisely 0.4 on a time scale of about 2 ps. Finally, $r(t=40$ fs, $T)$ remains at 2/5 independent of T, implying parallel pump and probe transition dipoles from 2 ps onward.

These results will be discussed later in the discussion in terms of dynamic modifications of the electronic structure of

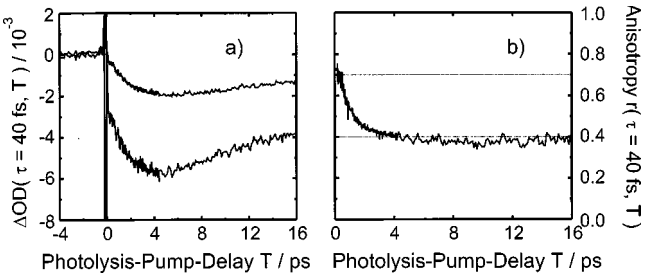

FIG. 9. (a) Pump-induced parallel and perpendicular optical densities as a function of photolysis-pump time delay T detected at a pump-probe delay τ of 40 fs. (b) Corresponding instantaneous anisotropy $r(\tau,=40$ fs, $T)$. Note that, at early times after photolysis, the instantaneous anisotropy exhibits a value of roughly 0.7, indicating the existence of higher lying electronic degeneracies involved in the pump and probe sequence. On a longer time scale, the anisotropy is constant and has a value of 0.4, indicating complete lifting of the electronic degeneracy beyond the spectral width of the pump and probe pulses with parallel pump and probe transition dipoles.

the system upon fragment recoil and approach of the asymptotic limit for two-body dissociation.

IV. DISCUSSION

A. Chirped wave packet dynamics

Excitation of triiodide at 400 nm induces nuclear motion which is initially directed along the symmetric stretching coordinate toward the transition state region for the bimolecular reaction of I_2^- with iodine radicals.[7,9,25,28,29] These dynamics are reflected in conventional pump-probe data in absorptive electronic transitions at early times whose temporal appearance is determined by the particular choice of probe wavelength. The probe wavelength defines the exact location of the detection window which is spanned on the symmetric stretching coordinate (see Fig. 2 and Ref. 9). The excess energy initially delivered by the 400-nm photolysis pulse amounts to roughly 1.5 eV with respect to the asymptotic limit for two-body dissociation if the iodine radical is formed in its spin-orbit ground state. Therefore, at early times before the passage through the transition state is completed, the wave packet has spectral components which cover both, bound and unbound, vibrational eigenstates of the future ground-state diiodide fragment. The unbound components will eventually be decelerated by solvent frictional forces and will ultimately collapse into the exit channel for diiodide formation. These dynamics lead to amplitude in the exit channel which is smeared out over a wide range of nuclear displacements along the future I_2^- coordinate. They are expected to contribute to the incoherent, nonoscillatory contributions observed in conventional pump-probe experiments. The bound components, on the other hand, will be forced to collapse into the exit channel by bouncing off the attractive portion of the reactive potential energy surface along the symmetric stretching coordinate. The anharmonicity in this direction, and the extent to which the solvent is able to randomly interact with this bound portion, strongly affects the resulting compactness of the I_2^- vibrational wave packet along the internuclear I_2^- distance. These combined effects determine the degree of product vibrational coherence (e.g., modulation depth) that can be observed experimentally in a conventional pump-probe setup. The first signature of this coherent portion of diiodide product formation is clearly detected below 300 fs as a pronounced shoulder on the falling edge of the early time transient absorption spike (see Fig. 2).[9] For probe wavelengths shorter than 700 nm, this shoulder presumably corresponds to those diatomic fragments whose bond is compressed for the first time after impulsive bond fission.[9] The subsequent periodic modulation of the conventional transient absorption simply reflects the bound motion of the remaining coherent superposition of diiodide vibrational eigenstates.

Section III A has demonstrated that a time-dependent product vibrational period appears in conventional pump-probe data. So-called ''chirped'' wave packet dynamics[30] can arise from either of the following three sources: (i) coherent and incoherent flow of vibrational excitation, (ii) nonstationary solvent-induced perturbations of the reactive po-

tential energy surface, and (iii) decay of residual interactions between the fragments.

Incoherent flow of vibrational excitation,[31,32] or vibrational relaxation, depends on the vibrational quantum number. For an oscillator bilinearly coupled to a bath, the state-to-state rate constants for transitions between vibrational eigenstates $|v'\rangle$ and $|v\rangle$ are proportional to the square of the matrix elements of the displacement operator $Q_{v'v}$. In case of a relaxing harmonic mode, these $|Q_{v'v}|^2$ increase linearly with quantum number v and the only nonvanishing elements are those for which $v'=v\pm1$. Anharmonicity leads to matrix elements $Q_{v'v}$, whose quantum number dependence is stronger than in the harmonic limit and, in addition, multiple quantum transitions become allowed. In addition, the individual rate constants are proportional to the amplitude of the frictional forces at the vibrational Bohr frequency $\omega_{v'v}$ of the relaxing mode. In general, these forces increase with decreasing frequency and, therefore, with increasing vibrational excitation of the anharmonic mode. Consequently, population relaxation from higher lying quantum states is much faster than near the bottom of the well.[10,11] A finite bandwidth probe laser selects a certain subset of eigenstates from the overall distribution of eigenstates that defines the vibrational wave packet. Faster population flow from higher lying quantum states within this subset as compared to lower ones may cause the wave packet frequency to increase with time due to anharmonic shifting of the vibrational period. This, however, requires a significant anharmonicity with respect to the energetic window defined by spectral bandwidth of the probe laser. Such a scenario has indeed been observed by Pugliano *et al.* in Block-type simulations of the time evolving density matrix of HgI, for which the anharmonicity is on the order of 1% of the harmonic frequency.[33,34] However, from gas phase potentials, it is known that the anharmonicity of diiodide is an order of magnitude smaller than for HgI. Therefore, we are tempted to conclude that incoherent flow of population does not contribute significantly to the chirped wave packet behavior of the nascent diiodide. However, we will come back to this interpretation later in the discussion.

In contrast to incoherent vibrational relaxation, coherent flow of population can also result in a time-dependent wave packet period.[34] For this mechanism to become effective a small anharmonicity is favorable. In this case, adjacent pairs of eigenstates have similar vibrational Bohr frequencies, resulting in nearly resonant transfer of population between these pairs with approximately equal state-to-state rate constants. Therefore, an initially prepared ensemble coherence will not be significantly perturbed since any loss of coherence due to downward transitions from a given level pair will be partially compensated for by additional downward transitions from an adjacent higher lying level pair until the relaxation is complete. This energy relaxation under retention of coherence can be visualized most clearly by a damped classical wave packed moving downward in a bound potential.[34] Evidence for participation of coherence transfer can be obtained from the experimental probe wavelength dependence of the dephasing time constant of the wave packet in comparison to simulations of the anharmonic energy relaxation in the coherent limit if the solvent forces acting on the oscillator are known. For I_2^- in liquid ethanol, we have recently established an individual rate constant for the $|1\rangle\leftarrow|0\rangle$ vibrational transition of 0.67 ps^{-1} in accord with previous results obtained by Barbara and co-workers.[7,10,11] Assuming a perfectly harmonic mode, this value extrapolates for higher quantum numbers around $v=10$ (which are selected by a probe wavelength of 580 nm, see Fig. 2) to dephasing times of about 300 fs. Referring to Fig. 2, this is also the phenomenological time scale that is experimentally observed at a probe wavelength of 580 nm. The expected behavior of the experimental dephasing time constants with probe wavelength indicates that a coherence transfer mechanism for population flow does not contribute significantly to the mechanism of vibrational relaxation of diiodide in ethanol solution. Thus, coherence transfer is unlikely to cause chirped wave packet dynamics of product diiodide ions as seen in conventional pump-probe data.

A further source of time-dependent vibrational wave packet periods is solvent-induced perturbations of the reactive potential energy surface that occur on time scales similar to those of the reactive nuclear motions themselves.[30] The elementary act of bond breakage may be accompanied by drastic changes of the charge distribution within the dynamically evolving system which, in turn, will induce a response of the surrounding solvent molecules. Dipolar or Coulombic solute-solvent coupling may result in an increase in the vibrational force constant of the potential along the nascent diatomic displacement. This is precisely what has been observed by Lim *et al.* for the impulsive photolysis of $HgBr_2$ in liquid dimethyl sulfoxide (DMSO) solution.[30] In this particular case, HgBr is initially formed in the local equilibrium solvent structure of its parent molecule and exhibits a vibrational frequency rather small compared to its gas phase value. Subsequently, the breaking of the parent solvation shell leaves the HgBr in an intramolecular potential characterized by the gas phase vibrational force constant. The breakup of the solvation shell leads to an extremely rapid decay of nuclear coherence on a time scale which is determined by the ultrafast components of intermolecular DMSO solvent degrees of freedom. Finally, the formation of a new solvent structure around the diatom can be monitored through chirped wave packet motion as the force constant decreases through solute-solvent coupling, with a continuing buildup of the equilibrated solvent environment around the product.[30]

The gas phase vibrational frequency of diiodide ions is 110 ± 2 cm^{-1}, which is close to the wave packet frequency observed experimentally for large photolysis-pump delays.[35] This agreement gives rather strong evidence for a solvation insensitive I_2^- force constant. Therefore, any rearrangements of the local solvent structure that may occur upon bond breakage of triiodide are highly unlikely to modify the product vibrational force constant. Hence, a time-dependent vibrational frequency of diiodide product ions after impulsive photolysis of triiodide is probably caused by pure solute motion, in particular, the dynamics of fragment separation in the liquid environment.

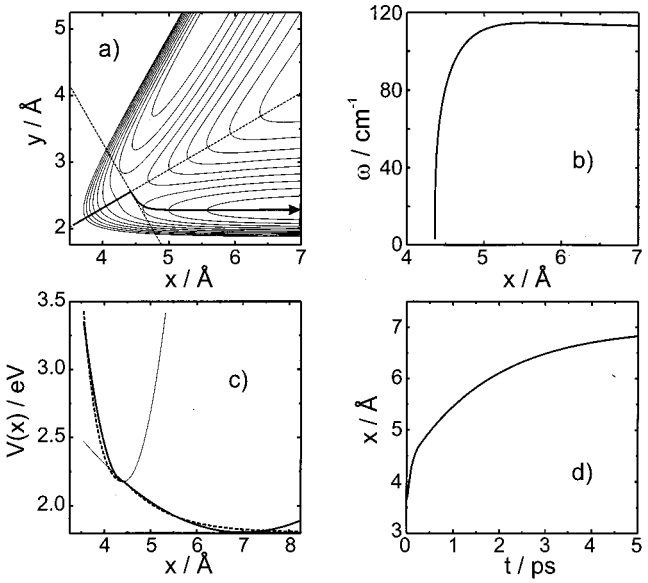

FIG. 10. Classical model for fragment recoil. (a) Contour plot of the empirical LEPS potential from Benjamin *et al.* as a function of Jacobi coordinates [see Eq. (4)]. The dashed lines indicate the symmetric and antisymmetric stretching coordinate, respectively. The solid arrow represents the direction of largest gradient that leads away from the initially prepared Franck-Condon region (see text). (b) Local diiodide frequency as a function of interfragment distance obtained from Eq. (5). (c) Cut through the LEPS potential along the direction of steepest descent projected onto the interfragment distance x (dashed curve). The solid curve represents a fit to this cut using piecewise harmonic potentials according to Eq. (6). The thin solid curves show the harmonic components to the fit. (d) Interfragment distance as a function of time obtained by solving Eq. (7) using the one-dimensional model potential from (c).

B. Classical model for fragment recoil

The masses of all atoms that participate in the photodissociation reaction of triiodide are fairly heavy, particularly when compared to those of the solvent molecules. This implies a classical behavior of the nuclear motion of the system during bond breakage. To model the recoil dynamics of the fragments in liquid solution, a potential energy surface (PES) is needed that describes the continuous motion from the initially prepared Franck-Condon region to the asymptotic limit of infinitely separated fragments. An empirical LEPS surface (London-Eyring-Polanyi-Sato) has been reported in the literature by Benjamin *et al.* for the fully collinear encounter of diiodide ions with iodine radicals.[36] This surface has the correct functional form in the asymptotic limit where the potential reduces to the known Morse potential of ground-state diiodide ions. The gradients of the potential in the Franck-Condon region have been optimized by fitting the liquid phase I_3^- absorption spectrum using classical trajectory calculations.[36] Figure 10(a) reproduces this two-dimensional surface for the fully collinear I_2^-/I encounter in Jacobi coordinates.[37] The latter are related to the two bond lengths r_1 and r_2 of the triatomic parent molecule through the relationships

$$x = ar_1 + br_2 \cos\theta \quad \text{and} \quad y = br_2 \sin\theta, \tag{4}$$

where $a = b = \sqrt{(2/3)}$ and $\theta = \pi/3$. The coordinate x corresponds to relative fragment translation, i.e., x equals the distance of the iodine radical from the center of mass of the diiodide fragment. The coordinate y is equal to the vibrational displacement of the future diiodide bond. The symmetric stretching coordinate is directed along an axis tilted by 30 deg with respect to x. The antisymmetric stretching coordinate is orthogonal to the symmetric mode.[8] A cut through the surface along the symmetric stretching direction is bound by about 0.73 eV with respect to total fragmentation. The minimum along this degree of freedom corresponds to a saddle point on the global surface and is called the transition state for the reaction $I_2^- + I$, i.e., the potential is unbound along the antisymmetric stretch. The curvature of the potential $V(x,y)$ along y calculated at the local equilibrium position $y_{eq}(x)$ is equal to the force constant $k(x)$ of the future diatomic bond at constant interfragment separation x. Therefore, the instantaneous frequency of the future diatomic fragment can be determined according to

$$k(x) = \left(\frac{\partial^2 V(x,y)}{\partial y^2} \right)_{x=\text{const}} \Bigg|_{y_{eq}} = [\mu 2\pi\omega(x)c]^2. \tag{5}$$

In Eq. (5), $\omega(x)$ is the vibrational frequency in cm^{-1} of the diiodide ion separated from an iodine radical by the distance x and c is the speed of light. The mass μ of the system represented in Jacobi coordinates is equal to the mass of an iodine atom.[8] It turns out that, directly at the transition state, the force constant for the diiodide bond at constant interfragment separation is nonzero, resulting in a local diiodide frequency of around 60 cm^{-1}. As the fragments begin to separate, the force constant (and hence, the local I_2^- frequency) increases rapidly with increasing x. For $x \to \infty$, the system approaches the asymptotic limit of the reaction and the local diiodide frequency assumes a value of 113 cm^{-1} corresponding to the harmonic frequency for equilibrated diiodide ions in bulk liquids,[25] as well as in supersonic jet expansions.[35] In other words, the force constant or, equivalently, the instantaneous diiodide frequency, is a direct measure of the interfragment separation for geometries ranging between the transition state region and the asymptotic limit for two-body dissociation. This interfragment distance dependence of the diiodide frequency basically reflects the magnitude of interactions between the fragments. As the fragments approach each other, a new bond between the central and the terminal atom is formed, thereby withdrawing electron density from the original diiodide ion. This weakens the original I_2^- bond and, in addition, decreases the frequency of the diatom. The x-dependence of the local I_2^- frequency is displayed in Fig. 10(b).

Therefore, we can conclude that chirped wave packet motion is indeed expected for the nascent diiodide ion unless the diatomic fragment reaches the asymptotic limit within less than a full vibrational cycle, i.e., the recoil dynamics is much faster than the equilibrium vibrational period of the product diatom. To model the recoil dynamics, we assume that the solute motion is much slower than that of the solvent. Consequently, fragment separation in the exit channel is hindered by a time-independent frictional drag. In addition, we decompose the reactive event on the global potential energy surface into motion along a nominal reaction coordi-

nate and vibration of the future diatomic product. The reaction coordinate is identified as the direction of steepest descent that leads to motion away from the initially prepared Franck-Condon region. At early times, this reaction coordinate carries exclusively symmetric stretching character. Once the transition state is reached, a finite displacement along the antisymmetric stretch ensures an asymmetric collapse of the triatomic system. The reaction coordinate continues to follow the largest gradient into the exit channels until it finally carries pure translational character for infinite times. The reaction coordinate is indicated in Fig. 10(a) by the solid arrow. A cut through the global PES along the reaction coordinate projected onto the interfragment distance x is shown in Fig. 10(c). We approximate this one-dimensional potential energy function by piecewise harmonic potentials according to

$$V_i(x)=\frac{1}{2}k_i(x-X_i)^2+E_i\,, \tag{6}$$

where $k_1=49.3$ kg/s for $x\leqslant(X_1=x_{\mathrm{TS}})$ and $k_2=1.8$ kg/s for $x>x_{\mathrm{TS}}$. The interfragment distance corresponding to the geometry of the transition state is denoted as x_{TS} and equals 4.427 Å. The parameter X_2 is adjusted to yield the best fit to the one-dimensional model potential in the exit channel region [$X_2=7$ Å, see Fig. 10(c)]. To further simplify the problem, the equation of motion on the potential (6) is simply written as

$$\mu_i\ddot{x}+\beta\dot{x}+k_ix=0. \tag{7}$$

A frictional force damps the evolution of the system along the interfragment distance, x, which is supposed to be of Stoke's type $F=6\pi\eta a v$ for each fragment. The velocities of the fragments are assumed to be equal and are denoted $v=\dot{x}/2$. The bulk viscosity of the solvent η is 1.1 cP for ethanol at room temperature.[38] Both hydrodynamic radii are set equal and are estimated from the known Lennard-Jones diameter of iodine radicals (2.15 Å).[39] It then follows that $\beta=3\pi a\eta$. Equation (7) describes the motion of a damped oscillator, whose time-dependent displacement x is plotted in Fig. 10(d). In combination with the distance dependence of the diiodide frequency discussed above, it is now possible to reconstruct the instantaneous vibrational frequency of the diiodide oscillator as a function of time after impulsive photolysis of triiodide in ethanol solution. Figure 11 shows a comparison of these simulations with the time dependence of the instantaneous vibrational frequency obtained from the resonance impulsive stimulated scattering data. Please note the logarithmic representation of the photolysis-pump-delay.

Surprisingly, we note that the low-frequency components rather than the fundamentals are in good agreement with the theoretical predictions of these classical model calculations. From this agreement, we draw the conclusion that the low-frequency oscillations observed in instantaneous resonance Raman scattering data arise from inner regions of the reactive potential energy surface with the reaction products in close proximity. Indeed, at very early photolysis-pump time delays, the resonance Raman response exhibits vibrational frequencies that agree very well with the local diiodide vibration of the system located in the vicinity of the transition state for the I_2^-/I reaction. In addition, the corresponding dephasing times of these frequency components are only 200 to 300 fs. They are consistent with an extremely rapid motion away from the inner regions of the potential energy surface that are interrogated by the pump pulse at the instant T. From the experimental data, the time scale for fragment recoil can be estimated. We conclude that it takes a minimum of 1 ps before all interactions between the fragments have decayed and the reaction products appear in the asymptotic limit.

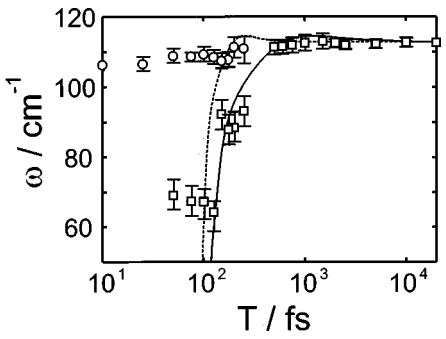

FIG. 11. Comparison of the vibrational frequencies predicted by the classical model (solid curve) and those obtained from instantaneous resonance Raman experiments (open symbols). The dashed curve reproduces the instantaneous vibrational frequency of the diiodide product in the limit of vanishing friction as predicted from quantum dynamics simulations.

Certainly, the considerations presented above are totally oversimplified. First, the model assumes that, during the recoil motion, the center of mass of the system is resting in the viscous fluid, as both fragments have been assigned the same mass and the same velocity. Second, any frequency dependence of the solvent frictional response is entirely neglected. Both assumptions can, in principle, be dropped by employing a proper Langevin or generalized Langevin-type description if the solvent forces acting at each point along the reaction coordinate are known.[1,2] It is important to keep in mind that, initially, the motion of the system is directed along the symmetric stretching coordinate, whereas, directly at the transition state, it is directed along the antisymmetric stretching coordinate. Once the system is fully collapsed, it moves exclusively along the interfragment distance. As pointed out by Hynes and co-workers for the barrier crossing aspect of atom transfer reactions, the random forces acting along these different reactive and nonreactive modes of the system should be distinctly different.[1] They can, however, be calculated from the individual forces on each atom that participates during the reactive motion in the vicinity of the transition state through transformation into the normal mode representation.[1]

Furthermore, the model reduces the recoil dynamics to the perfectly collinear geometry. This assumption is rather questionable since the importance of the bending coordinate at early times of the reaction has previously been pointed out.[14] Finally, the classical model also neglects the spreading of amplitude that occurs at very early times due to the finite duration of the excitation pulse.[9,40] The simple model calculations may only give a reasonable picture for those spectral components of the early time wave packet which initially

cover the set of unbound eigenstates of the future diiodide fragment. Bound portions are reflected off the attractive wall of the potential energy surface along the symmetric stretching coordinate and will, therefore, appear in the asymptotic limit much earlier. Furthermore, at such early stages of the reaction, they may not experience the same spectrum of frictional forces as the unbound portion of the wave packet, which is able to cover a relatively flat region of the PES mostly along the symmetric stretching coordinate. It is in this region where the system's nuclear motion at early times becomes most susceptible to solvent frictional forces, although the simple one-dimensional calculation does not consider dynamics at such large symmetric displacements.

We previously published quantum dynamics simulations on the full two-dimensional LEPS potential for excitation at 400 nm.[9] These can be used to estimate a mean time-dependent interfragment separation in the limit of vanishing frictional drag by calculating the first moment of the full two-dimensional wave packet projected onto the interfragment coordinate *x*. The resulting time dependence of the diatom frequency is reproduced in Fig. 11 as the dashed curve. Indeed, one can see that the pure quantum evolution predicts the appearance of the fundamental frequency of equilibrated diiodide ions already for delays as short as 200 fs. The fact that the fundamental frequency is experimentally observed for even shorter photolysis-pump delays well below 50 fs can then be explained qualitatively by the enormous spreading that the wave packet experiences already within the duration of the photolysis pulse (see also Refs. 9 and 40).

Ruhman and co-workers were able to demonstrate transient resonance impulsive stimulated Raman scattering in liquids for the first time.[15,16] They also performed experiments on diiodide ions following impulsive photolysis of triiodide in ethanol solution at 308 nm. In their studies, an increase of the instantaneous vibrational frequency of diiodide from 102 to 113 cm^{-1} for photolysis-pump delays ranging between 2 and approximately 15 ps was observed.[15,16] It was concluded that this time-dependent vibrational frequency reflects the dynamics of vibrational thermalization of the product diatoms rather than fragment separation. In the studies reported here with excitation at 400 nm, we observe much larger shifts of the vibrational frequency from 65 to 113 cm^{-1}. These major changes occur on time scales well below 2 ps after impulsive photolysis. For delays larger than 2 ps, the frequency of the diiodide fragment remains more or less constant within the accuracy of the experiment. Yet for 2 ps onward, the dynamics of vibrational thermalization can unambiguously be identified through the time dependence of the incoherent absorption spectrum of diiodide.[7]

To briefly summarize, the time window below 2 ps is obviously characterized by three distinctly different experimental observations: (i) a pronounced temporal rise of the overall transient absorption observed in conventional pump-probe data which is independent of the probe wavelength. (ii) Product vibrational coherences in conventional pump-probe that reveal chirped wave packet motion. (iii) Dramatic changes of the instantaneous I_2^- frequency extracted from instantaneous resonance Raman scattering. Since all these features occur on the same time scale, it seems plausible to assign them to the same dynamical process. Since chirped wave packet dynamics can be explained by neither coherent nor incoherent flow of vibrational population as discussed previously, it is indeed very likely that fragment separation dictates the time scale below 2 ps.

So far, we have based our discussion only on experiments that probe scalar properties of the system as it evolves from the initial Franck-Condon region toward the region of well separated fragments. Further support for the idea that recoil dynamics dominates the time window below 2 ps stems from the instantaneous anisotropy experiments presented above. These experiments give insight into purely electronic properties of the dynamically evolving system[17,18] which should remain unaffected by the dynamics of vibrational relaxation. As in any kind of chemical reaction, the dynamic evolution of the system during the process of bond breakage is made possible through electronic correlations that connect reactants (i.e., the Frank-Condon region) with the asymptotic limit of well separated products. Therefore, detecting purely electronic properties of the system during the course of bond fission is a more direct probe to access the dynamics of fragment recoil and, in addition, is uncontaminated by the dynamics of vibrational relaxation.

C. Instantaneous coherent anisotropies

In Sec. III C it was shown that the initial anisotropy for very short photolysis-pump delays can exceed the theoretical value of 0.4 expected for parallel pump and probe transition dipoles. A maximum value of 0.7 has been observed around $T=0$. With increasing T the anisotropy at constant τ decays to the predicted value of 0.4 on a time scale of about 2 ps. An anisotropy of 0.7 is indicative of electronic degeneracies involved in the pump-probe sequence.[17,18] The pump pulse interrogates the system which has been allowed to evolve on the reactive potential for the time T. It creates an electronic coherence between two degenerate higher lying states whose individual transition dipole moments are orthogonal with respect to each other.[17,18] The probe pulse couples both components of this electronically coherent superposition to a common final state, in particular, back to the reactive potential energy surface. The electronic coherence decays along the pump-probe time delay within a few tens of femtoseconds due to random interactions of the chromophore with the surrounding solvent (dephasing). As the T-delay is increased at constant pump-probe time delay, the fragments separate and their interactions begin to decay. Concurrently, the higher lying electronic degeneracy is gradually lifted and the energy splitting begins to exceed the pump and probe laser spectral bandwidth. As discussed extensively by Wynne and Hochstrasser, one can describe the anisotropy phenomenologically as a sum of an incoherent contribution due to population of the degenerate electronic states and a coherent contribution due to the interference of the two components that comprise the electronic superposition state,[17,18]

$$r(\tau,T)=\frac{1}{10}\{4+3\cos[\Delta(T)\tau]\exp(-\Gamma_2\tau)\}. \tag{8}$$

The former contributes with the well known amplitudes of 0.4 which is predicted for parallel pump and probe transition dipoles. The latter gives rise to an additional amplitude of 0.3 for vanishing energy splitting Δ and dephases along τ with a phenomenological rate constant of Γ_2. The electronic coupling Δ is a function of the interfragment distance and, therefore, depends implicitly on the photolysis-pump delay T. The anisotropy shown in Fig. 9 decays roughly exponentially along T with a time constant of 600 fs. Furthermore, a sub-picosecond time constant is in good agreement with the time scale for fragment recoil deduced from the instantaneous resonance Raman data of the diiodide vibrational frequency.

Again, the agreement of time scales between two independent experiments (i.e., instantaneous resonance impulsive stimulated scattering and instantaneous anisotropy) indicates that they reflect the very same dynamic, namely the decay of fragment interactions due to recoil motion on the reactive potential energy surface. To reiterate, the process of vibrational relaxation is not expected to change the electronic structure of the system. Finally, the time constant of the decay of $r(\tau,T)$ along T agrees perfectly with the time constant observed for the wavelength-independent rising component of the transient absorption observed in conventional pump-probe experiments. From all findings presented in this paper, one can conclude that the dynamics of fragment separation takes place on a time scale of approximately 2 ps. Furthermore, we can also conclude that chirped wave packet motion as seen in conventional pump-probe experiments on photodissociating triiodide ions in liquid solution essentially reflects the dynamics of fragment recoil and the concomitant decay of fragment interactions that perturb the potential energy surface along the vibrational coordinate of the future diatomic fragment.

From the anisotropy data shown in Fig. 9, the time-dependent electronic coupling can, in principle, be determined. This, in turn, can be used to construct potential energy functions along the interfragment distance x for the higher lying electronic state manifold via Eq. (9) in combination with one-dimensional model simulation. The nature of these states, however, remains unclear and we refrain at this point from such an analysis. Yet, in the asymptotic limit, it is known that absorptive near-infrared transitions from the reactive surface are assigned to the $(^2\Pi_g \leftarrow ^2\Sigma_u^+)$ resonance of I_2^-.[21,41–43] This resonance corresponds to a perpendicular transition in the molecular frame of the product diatom. Another electronic resonance that originates from the asymptotic limit corresponds to $(^2\Sigma_g^+ \leftarrow ^2\Sigma_u^+)$, which is a parallel transition in I_2^-. Since the transition dipoles of the degenerate electronic states in the vicinity of the transition state region need to be perpendicular, it is tempting to conclude that the correlate directly with electronic states of Σ and Π symmetry of the product diatom in the asymptotic limit. A full interpolation of these electronic correlations, including an assignment from the instantaneous anisotropy data presented here is, however, entirely subject to speculation at this point.

V. CONCLUSION

The time scale for fragment recoil in the femtosecond photodissociation of triiodide in solution has been explored by means of two independent experiments: instantaneous resonance impulsive stimulated scattering and instantaneous anisotropy. The former experiment essentially detects the local frequency of the diatom as a function of time after impulsive photolysis of the triatomic parent ion. The latter, on the other hand, probes exclusively electronic properties of the system as it moves from the initially prepared Franck-Condon region of the parent species through the transition state toward the region of spatially well separated fragments. However, both experiments reveal the same dynamics of recoil through the concurrent decay of interactions between the fragments. From the agreement between both sets of experiments, we estimate a time scale for product separation in liquid ethanol solution of about 2 ps.

Further experiments are currently in progress in order to explore recoil dynamics in a variety of different solvents. This gives valuable insight into interesting aspects of the dissociation reaction that are related to the influence of solvent-induced symmetry breaking on the dynamics of fragment separation. In addition, a pronounced excitation energy dependence has previously been found from conventional pump-probe studies. Photodissociation at 266 nm initiates the bond fission purely on a higher lying electronic configuration of triiodide. In this case, bond breakage is also a direct process leading to diiodide ions in its electronic ground state $^2\Sigma_u^+$ and presumably spin-orbit excited iodine radicals. The instantaneous anisotropy following impulsive 266-nm photolysis should yield important additional information regarding the electronic structure of the I_3^-/I_2^- system and, in particular, the electronic correlations that facilitate the fundamental process of bond fission.

ACKNOWLEDGMENT

Financial support by the Deutsche Forschungsgemeinschaft (SFB 357: ''Molekulare Mechanismen Unimolekularer Reaktionen,'' SFB 195: ''Elektronen in Mikroskopischen und Makroskopischen Systemen,'' and Schwerpunktprogramm ''Femtosekundenspektroskopie elementarer Anregungen in Atomen, Molekülen und Clustern'') is gratefully acknowledged.

APPENDIX

The number density of molecules on the reactive potential energy surface (PES) before the instant of the pump at time $t<T$ is given by n_0. The pump pulse at time $t=T$ is polarized along the z-axis and excites the molecules with a probability proportional to $\cos^2\theta$, where θ is the angle between pump polarization and pump transition dipole moment. The excitation leaves an anisotropic distribution of molecules on the reactive PES which spatially randomizes with time according to $F_{\mathrm{rot}}(\tau)$, where τ is the pump-probe time delay. The recovery of the reactive PES (e.g., at infinite T, through photodissociation/geminate recombination of the

diatom) is governed by the function, $K(\tau)$. The number density of molecules on the reactive PES as a function of τ is therefore proportional to

$$n_g(\tau,\phi,\theta)=\frac{1}{4\pi}\{n_0-nK(\tau)[(3\cos^2\theta-1)F_{\rm rot}(\tau)+1]\}, \tag{A1}$$

where n is the number density of molecules excited by the pump. Furthermore, the optical density on the probe field at delay, τ, is proportional to the scalar product of the probe transition dipole and probe polarization. In the case of degenerate pump and probe transition dipoles, μ, one finds a pump-induced optical density of

$$\Delta{\rm OD}(\tau)=\int_0^{2\pi}d\phi\int_0^{\pi}d\theta\sin\theta(\mathbf{u}\cdot\mathbf{e}_{\rm Probe})^2[n_g(\tau,\phi,\theta)-(1/4\pi)n_0]. \tag{A2}$$

Therefore, pump-induced optical densities detected with probe light polarized parallel and perpendicular with respect to the pump polarization are proportional to $\cos^2\theta$ and $\sin^2\theta$, respectively,

$$\Delta{\rm OD}_{\parallel}(\tau)=2\pi\int_0^{\pi}d\theta\sin\theta\cos^2\theta|\boldsymbol{\mu}|^2[n_g(\tau,\phi,\theta)-(1/4\pi)n_0], \tag{A3}$$

$$\Delta{\rm OD}_{\perp}(\tau)=\pi\int_0^{\infty}d\theta\sin^3\theta|\boldsymbol{\mu}|^2[n_g(\tau,\phi,\theta)-(1/4\pi)n_0]. \tag{A4}$$

As indicated in Sec. III C, the anisotropy can display singularities for very short photolysis-pump time delays, T. As already mentioned, such a behavior reflects a time-dependent absorption cross section σ of the system as the fragments of the I_3^- photodissociation begin to separate. Let $|\boldsymbol{\mu}|^2$ be proportional to $\sigma(\tau)$ and insert Eq. (A1) into Eqs. (A3) and (A4), and one obtains

$$\Delta{\rm OD}_{\parallel}(\tau,T)=\frac{1}{3}\left\{[\sigma(\tau)-\sigma_0]n_0-\sigma(\tau)n\times\left[1+\frac{4}{5}F_{\rm rot}(\tau)\right]K(\tau)\right\}, \tag{A5}$$

$$\Delta{\rm OD}_{\perp}(\tau,T)=\frac{1}{3}\left\{[\sigma(\tau)-\sigma_0]n_0-\sigma(\tau)n\times\left[1-\frac{2}{5}F_{\rm rot}(\tau)\right]K(\tau)\right\}, \tag{A6}$$

where $\sigma_0=\sigma_0(T)$ represents the absorption cross section at the instant of the pump, T (i.e., $\tau=0$). Thus, the anisotropy, $r(\tau,T)$, is given by

$$r(\tau,T)=\frac{2}{5}F_{\rm rot}(\tau)\frac{1}{1-\dfrac{[\sigma(\tau)-\sigma_0]n_0}{\sigma(\tau)nK(\tau)}}, \tag{A7}$$

and the magic angle transient can be written as

$$\Delta{\rm OD}_{54.7}(\tau,T)=[\sigma(\tau)-\sigma_0]n_0-\sigma(\tau)nK(\tau). \tag{A8}$$

Equations (A5) through (A8) have the correct functional form if the temporal dependence of σ disappears [i.e., $\sigma(\tau)=\sigma_0$]. In the case of an increasing cross section (e.g., due to separation of the fragments on the reactive PES), both $\Delta{\rm OD}_{\parallel}$ and $\Delta{\rm OD}_{\perp}$ experience a sign change displaying a transient bleach at early τ-delays and a transient absorption for large τ. The same behavior is observed for the magic angle transient at a delay for which the condition

$$\frac{\sigma(\tau)-\sigma_0}{\sigma(\tau)}=\frac{n}{n_0}K(\tau) \tag{A9}$$

is fulfilled. Consequently, the anisotropy passes through a singularity at precisely this delay [see also Eq. (A7)]. It is important to note, however, that regardless of the τ-dependence of σ, $r(\tau\rightarrow 0,T)$ still approaches a value of 0.4 since $\sigma(\tau)\rightarrow\sigma_0$ and pump and probe transition dipoles are parallel with respect to each other.

We crudely estimate the kinetic term, $K(\tau)$, from an independent measurement of the instantaneous Raman/bleach response at infinite T which can be described reasonably well by a double-exponential decay due to recombination-induced ground-state recovery of diiodide ions

$$K(\tau)=A_1\exp(-\tau/\tau_1)+A_2\exp(-\tau/\tau_2). \tag{A10}$$

Here, the parameters are given by $A_1=0.51$, $A_2=0.49$, $\tau_1=22.7$ ps, and $\tau_2=1.84$ ps. Analogously, the rotational decay term, $F_{\rm rot}(\tau)$, obeys the following form:

$$F_{\rm rot}(\tau)=B_1\exp(-\tau/\tau_{r1})+B_2\exp(-\tau^2/\tau_{r2}^2), \tag{A11}$$

and is estimated from the corresponding anisotropy at infinite T. The parameters for the diffusive contribution are $B_1=0.6$ and $\tau_{r1}=9.5$ ps. The inertial contribution is defined by $B_2=0.4$ and $\tau_{r2}=1.1$ ps. For the functional form of $\sigma(\tau)$ we choose an exponential according to

$$\sigma(\tau)=\sigma_\infty-(\sigma_\infty-\sigma_0)\exp(-\tau/\tau_\sigma). \tag{A12}$$

Arbitrarily setting σ_0 to unity leaves the relative cross section of equilibrated diiodide ions, σ_∞, and the time constant, τ_σ, as the only adjustable parameter for a given initial bleach n/n_0

As an example, we set $n/n_0=0.1$. With $\sigma_\infty/\sigma_0=1.042$ and a time constant, τ_σ, of 2.5 ps, it is possible to quantitatively reproduce both pump-induced optical densities and the anisotropy, $r(\tau,T)$, as demonstrated in Fig. 8 for a photolysis-pump delay of 500 fs. In addition, the time constant, τ_σ, is in very good agreement for the time scale associated with fragment recoil. Therefore, we conclude here that the transition moment for absorptive resonances from the reactive PES increases with increasing separation of the fragments in the triiodide photodissociation.

[1] J. T. Hynes, in *The Theory of Chemical Reaction Dynamics*, edited by M. Baer (CRC, Boca Raton, 1984), Vol. 4, pp. 171.
[2] P. Hänggi, P. Talkner, and M. Borkovec, Rev. Mod. Phys. **62**, 251 (1990).
[3] G. R. Fleming, T. Joo, and M. Cho, Adv. Chem. Phys. **101**, 141 (1997).
[4] G. R. Fleming and M. Cho, Annu. Rev. Phys. Chem. **47**, 109 (1996).
[5] W. P. de Boeij, M. S. Pshenichnikov, and D. A. Wiersma, Annu. Rev. Phys. Chem. **49**, 99 (1998).
[6] U. Banin and S. Ruhman, J. Chem. Phys. **98**, 4391 (1993).
[7] T. Kühne and P. Vöhringer, J. Chem. Phys. **105**, 10788 (1996).

[8] G. Ashkenazi, U. Banin, A. Bartana, R. Kosloff, and S. Ruhman, Adv. Chem. Phys. **100**, 229 (1997).
[9] T. Kühne, R. Küster, and P. Vöhringer, Chem. Phys. **233**, 161 (1998).
[10] P. K. Walhout, J. C. Alfano, K. A. M. Thakur, and P. F. Barbara, J. Phys. Chem. **99**, 7568 (1995).
[11] D. A. V. Kliner, J. C. Alfano, and P. F. Barbara, J. Chem. Phys. **98**, 5375 (1993).
[12] A. E. Johnson and A. B. Myers, J. Phys. Chem. **100**, 7778 (1996).
[13] E. Gershgoren, E. Gordon, and S. Ruhman, J. Chem. Phys. **106**, 4806 (1997).
[14] T. Kühne and P. Vöhringer, J. Phys. Chem. **102**, 4177 (1998).
[15] U. Banin, R. Kosloff, and S. Ruhman, Chem. Phys. **183**, 289 (1994).
[16] U. Banin and S. Ruhman, J. Chem. Phys. **99**, 9318 (1993).
[17] K. Wynne and R. M. Hochstrasser, J. Raman Spectrosc. **26**, 561 (1995).
[18] K. Wynne and R. M. Hochstrasser, Chem. Phys. **171**, 179 (1993).
[19] H. Isci and W. R. Mason, Inorg. Chem. **24**, 271 (1985).
[20] V. Herrmann and P. Krebs, J. Phys. Chem. **99**, 6794 (1995).
[21] E. C. M. Chen and W. E. Wentworth, J. Phys. Chem. **89**, 4099 (1985).
[22] W. T. Pollard, S.-Y. Lee, and R. A. Mathies, J. Chem. Phys. **92**, 4012 (1990).
[23] H. Barkhuijsen, R. De Beer, W. M. M. J. Bovee, and D. van Ormondt, J. Magn. Reson. **61**, 465 (1985).
[24] F. W. Wise, M. J. Rosker, G. L. Millhauser, and C. L. Tang, IEEE J. Quantum Electron. **QE-23**, 1116 (1987).
[25] A. E. Jonhson and A. B. Myers, J. Chem. Phys. **102**, 3519 (1995).
[26] S. Hess and P. Vöhringer, in *Ultrafast Phenomena XI*, edited by T. Elsaesser, J. G. Fujimoto, D. A. Wiersma, and W. Zinth (Springer Verlag, New York, 1998), p. 600.
[27] M. Volk, S. Gnanakaran, E. Gooding, Y. Khodolenko, N. Pugliano, and R. M. Hochstrasser, J. Phys. Chem. **101**, 638 (1997).
[28] U. Banin, A. Bartana, S. Ruhman, and R. Kosloff, J. Chem. Phys. **101**, 8461 (1994).
[29] A. E. Johnson and A. B. Myers, J. Chem. Phys. **104**, 2497 (1996).
[30] M. Lim, M. F. Wolford, P. Hamm, and R. M. Hochstrasser, Chem. Phys. Lett. **290**, 355 (1998).
[31] J. Chesnoy and G. M. Gale, Adv. Chem. Phys. **70**, 297 (1988).
[32] J. C. Owrutsky, D. Raftery, and R. M. Hochstrasser, Annu. Rev. Phys. Chem. **45**, 519 (1994).
[33] N. Pugliano, A. Z. Szarka, S. Gnanakaran, and R. M. Hochstrasser, J. Chem. Phys. **103**, 6498 (1995).
[34] N. Pugliano, A. Z. Szarka, and R. M. Hochstrasser, J. Chem. Phys. **104**, 5062 (1996).
[35] M. T. Zanni, T. R. Taylor, B. J. Greenblatt, B. Soep, and D. M. Neumark, J. Chem. Phys. **107**, 7613 (1997).
[36] I. Benjamin, U. Banin, and S. Ruhman, J. Chem. Phys. **98**, 8337 (1993).
[37] R. Schinke, *Photodissociation Dynamics* (Cambridge University Press, Cambridge, 1993).
[38] *CRC Handbook of Chemistry and Physics*, edited by R. C. Weast (CRC, Boca Raton, 1983), Vol. 64.
[39] B. Otto, J. Schroeder, and J. Troe, J. Chem. Phys. **81**, 202 (1984).
[40] G. Ashkenazi, R. Kosloff, S. Ruhman, and H. Tal-Ezer, J. Chem. Phys. **103**, 10005 (1995).
[41] B. J. Greenblatt, M. T. Zanni, and D. M. Neumark, Science **276**, 1675 (1997).
[42] J. M. Papanikolas, J. R. Gord, N. E. Levinger, D. Ray, V. Vorsda, and W. C. Lineberger, J. Phys. Chem. **95**, 8028 (1991).
[43] D. Ray, N. E. Levinger, J. M. Papanikolas, and W. C. Lineberger, J. Chem. Phys. **91**, 6533 (1989).